

Cover Page



Universiteit Leiden



The handle <http://hdl.handle.net/1887/22291> holds various files of this Leiden University dissertation.

Author: Snel-Bongers, Jorien

Title: Dual electrode stimulation in cochlear implants : from concept to clinical application

Issue Date: 2013-11-20

Chapter 3

The use of partial bipolar stimulation in cochlear implants to create spectral channels apical to the stimulated electrode pair

J Snel-Bongers, JJ Briaire, RK Kalkman, W Nogueira, FJ Vanpoucke, JHM Frijns

Ear and Hearing, submitted

Abstract

Objectives: Cochlear implant electrode arrays have a more shallow insertion depth than the physiological place-to-frequency distribution, as a deep insertion could lead to intra-cochlear trauma. An alternative for a deeper insertion can be the so-called phantom channel, which is partial bipolar stimulation, with non-equal amplitudes on the two stimulating contacts. Through the use of psychophysical experiments and computational modeling this study investigates the neural excitation, place of stimulation and the perceived loudness of a phantom channel.

Design: Ten postlingually adult deafened users of the HiRes90K cochlear implant with a HiFocus1J electrode array were selected to participate in this study. The stimulation level required to maintain equal loudness with monopolar stimulation was determined with a psychophysical loudness balancing experiment. The largest achievable pitch shift by varying the bipolar coefficient was determined in two steps, using a pitch-ranking procedure followed by a pitch matching experiment. Through use of a computational model of the cochlea, the mechanism underlying phantom stimulation was studied, predictions concerning the current correction required to reach similar excitation widths and the largest pitch shift for three different cochlear morphologies with the electrode array in both medial and lateral position.

Results: (1) More current is needed on the primary electrode when increasing the current on the compensating electrode to maintain equal loudness. (2) All subjects exhibited an apical pitch shift with an average of 1 electrode contact. (3) The psychophysical results are in line with the predictions of the computational model. (4) The computational model predicts that the electrode array in lateral position exhibits a larger pitch shift to apical than the medial position.

Conclusion: Both the computational model of the cochlea and the psychophysical data show that it is possible to stimulate in a more apical region with phantom stimulation and that more current is needed to maintain equal loudness. The model predicts, however, that stimulating at lower levels decreases the pitch shift and the electrode array in a lateral position would generate a larger pitch shift than in medial position.

Introduction

Cochlear implants (CIs) are widely used as a treatment for profoundly hearing impaired children and adults. There is some evidence that speech recognition by implant users is improved when the acoustic input frequency is matched to the cochlear location that normally processes that frequency range (Baskent and Shannon 2004). However, if an electrode array does not span the desired frequency range, which is the case in the CI types of Advanced Bionics and Cochlear (typical length of standard electrode arrays 18-24 mm, extending up to maximal 1 ½ turns of the cochlea), a matched map would result in the loss of low frequency information (Carlyon et al. 2010). One way to resolve this issue is a deeper insertion into the cochlea. The electrode arrays used in Med-EL devices can be considerably longer than the arrays from other manufacturers, following the concept of full cochlear coverage. Their standard arrays are 28 to 31 mm long, which is almost the complete length of the basilar membrane. Recent studies have shown the transmission of very low frequency information, either electrically or acoustically, can improve speech perception scores from implant users in general (Dorman et al. 2005; Gantz and Turner 2004; Gantz et al. 2004; Riss et al. 2011; Turner et al. 2008; von Ilberg et al. 2011; von et al. 1999). However, when most currently available electrode arrays are inserted very deeply into the cochlea they tend to produce more intra-cochlear trauma, with placement of the electrode array in the scala vestibuli instead of the scala tympani, loss of residual hearing and reduction of the neural substrate (Boyd 2011). Skinner et al. (2007) and Finley et al. (2008) showed that misplacement in the scala vestibuli or deep insertion have a negative influence on speech perception, leading to the use of shorter arrays to reduce possible trauma. Another way to reach the apical region is by stimulating electrically beyond the position of the physical electrode array. Phantom electrodes (Saoji and Litvak 2010) or pseudo-monophasic pulses (Macherey et al. 2011) are examples of such stimulation in the more apical region and probably can both be an alternative to a deeper electrode array insertion. Similarly, it is also possible to stimulate in the more basal direction, when an electrode array is over inserted.

A phantom channel is a form of partial bipolar stimulation, with non-equal amplitudes on the two stimulating contacts (Saoji and Litvak (2010)). A biphasic pulse (cathodic – anodic) is presented on the apical electrode contact, also called “primary” electrode. An out-of-phase biphasic pulse (anodic – cathodic) with lower amplitude is presented on the adjacent basal electrode contact, also called “compensating” electrode. The ratio between amplitudes of the compensating

electrode and the primary electrode is termed σ . This means that when $\sigma = 0$, only the primary electrode is stimulated (as in a monopolar configuration), and when $\sigma = 1$, stimulus levels of the primary and compensating electrodes are equal, as in bipolar stimulation.

Because the currents to the neighboring contacts are applied out of phase, the intracochlear electrical field is pushed away from the compensating electrode, to the other side of the primary electrode (Saoji and Litvak 2010). This makes it possible to create spectral channels beyond the electrode array. Saoji and Litvak (2010) showed that it is possible to shift the percept from 0.5 to 2 contact spacings beyond the primary electrode.

Another way to stimulate beyond the electrode array is with pseudo-monophasic pulses (Macherey et al. 2011). Here two electrodes were stimulated in a bipolar fashion with an initial short, high-amplitude anodic phase (relative to the most apical electrode) followed by a long, low-amplitude phase of opposite polarity. This resulted in a place pitch shift between 0.55 and 1.1 mm (0.5 to 1 electrode contacts) in an apical direction.

To supplement clinical data, simulations of phantom electrode excitation were performed using a computational model of the implanted human cochlea. The model (Briaire and Frijns 2000; Briaire and Frijns 2005; Briaire and Frijns 2006; Frijns et al. 2001; Frijns et al. 2009a; Frijns et al. 2009b) provides insight into CI-induced electrical potential distributions and their resulting neural excitation patterns in a three-dimensional human cochlear geometry. By simulating the psychophysical experiments and objective measures of CI recipients, an electro-anatomical model can therefore shed light on the internal workings of new excitation strategies such as phantom electrode stimulation.

Most studies are currently performed at most comfortable loudness (MCL) level, as in the study by Saoji and Litvak (2010). A recent study from Snel-Bongers et al. (2013) showed that when current steering is performed near threshold level (TL), the current compensation needed to maintain equal loudness is different than at MCL level. Using computational modelling, Frijns et al. (2009b) showed differences in excitation profiles between current steering at MCL and at TL. This study will investigate the effect of lower stimulation levels on a phantom electrode using computational modeling.

To summarize, in this study the phantom stimulation technique has been investigated. The following issues are addressed: 1) the stimulation level to maintain equal loudness; 2) the σ with the largest pitch shift in apical direction and

the size of this shift; 3) the consistency between psychophysical data and computational modeling; 4) the influence of the position of the electrode array; 5) the effect of lower stimulation level on the size of the shift.

Method

Subjects

A group of 10 postlingually deafened adults was recruited. All were unilaterally implanted at the LUMC in the period between 2002 and 2007 and received a HiRes90k implant with a HiFocus-1j electrode array (Advanced Bionics, Valencia, CA). No problems were reported during surgery or the subsequent rehabilitation program. Subject information is provided in Table 1. All subjects achieved a phoneme recognition score above 50%, obtained with the standard Dutch speech test from the Dutch Society of Audiology (Bosman and Smoorenburg 1995). Written informed consent was obtained before any study procedures were conducted. This study was approved by the Medical Ethical Committee of the LUMC under number P02.106.M.

Table 1. Subject demographics.

	Gender	Age (years)	Aetiology	Duration of deafness (years)	CI side	CI usage (months)	CVC Ph%	Electrodes tested	
								180°	360°
S1	Female	59	Familiar progressive	29	left	54	87	10	3
S2	Male	58	Unknown	3	right	48	86	12	5
S3	Male	56	Loudness	4	right	73	84	13	6
S4	Female	70	Familiar progressive	10	right	30	91	10	4
S5	Male	46	Familiar progressive	16	right	60	95	11	4
S6	Female	48	Familiar progressive	30	right	38	65	10	4
S7	Female	44	Congenital	36	right	37	86	11	5
S8	Female	58	Congenital	10	right	38	77	9	2
S9	Female	56	Rubella intra uterine	50	right	40	66	11	5
S10	Female	59	Unknown	50	left	45	54	11	4
Average		55		23		46			

Speech perception scores are given as percentage phonemes correct (Ph%) in phonetically balanced monosyllabic (CVC) words.

Assessment of Electrode location

The intracochlear position of the all electrode contacts was determined from a postoperative CT-scan which is administered as part of the clinical CI program. To measure the exact position of the electrode contacts, a Multiplanar reconstruction (MPR) was made from the CT-scan (Verbist et al. 2005). A system of coordinates, described in previous papers (Snel-Bongers et al. 2011; Snel-Bongers et al. 2012), was applied to the postoperative MPR using a custom Matlab application (MathWorks, Natick, MA). All electrode contacts were marked by an experienced physician. In accordance with the consensus on cochlear coordinates, the angles used in this study were calculated with the round window as the 0° reference (Verbist et al. 2010a; Verbist et al. 2010b). To control for variation in insertion depth and in cochlear dimensions, electrode contacts at the same rotational angle were selected for test. For each subject the electrode contact closest to 360° (apical site, AS) and the one closest to 180° (basal site, BS) were selected from the electrode array (Table1) and used in the following experiments. Although the infra apical stimulation is of interest, the experiments were performed on electrodes in the middle of the electrode array. This made it possible to perform the experiments at the same location for each subject and to compare the pitch produced by phantom with that produced by current steering.

Psychophysical experiments

The psychophysical experiments were performed with PACTS (PsychoACoustic Test Suite, Advanced Bionics Europe, Niel, Belgium) and the BEDCS (Bionic Ear Data Collection System, Advanced Bionics, Valencia, CA) research tool for the electrical stimulus configuration. Stimuli were bursts of biphasic pulses with phase duration of 32.32 μ s, pulse rate of 1,400 pulses per second and total burst duration of 300 msec. A pause of 300 msec was inserted between stimulus bursts.

With Current Steering (CS), stimuli were simultaneous and in-phase, applied on adjacent electrode contacts. The proportion of the total current directed to the more basal contact of the stimulated pair is denoted as α . This coefficient varies from $\alpha = 0$, where all current is directed to the apical electrode (AS or BS) to $\alpha = 1$, where all current is directed to the basal electrode (Donaldson et al. 2005). For phantom stimulation, stimuli were also simultaneous, but out of phase, also applied on two adjacent electrode contacts. The apical electrode was used as the primary electrode, or the stimulating electrode, while a basal electrode was used as the compensating electrode. The ratio of the current magnitude applied to the

compensation electrode divided by that applied to the primary electrode is denoted by compensation coefficient σ (Saoji and Litvak 2010).

The output current of the implant device is limited by the voltage compliance limit of the internal electronics. To characterize the actual stimulation in the patients at levels above compliance the current sources of the HiRes90K implant were scrutinized by recording the output voltage of a clinical implant with a microprobe at the electrode contact. The current sources demonstrated a linear behavior right up to the saturation level (7.13 V with a load of 5kOhm). Specifying higher output levels does not change the actual output, it stays at this saturation level. It also turned out that the amplitude of the first half of the pulse phase is up to 2.6% higher than that of the second half. This phenomenon, occurs however, also with pulses below saturation level (1.2% on average, without a clear trend with respect to stimulation level). This relative stable pulse shape and the fixed output charge makes it a valid approach to use the saturation current as output level for current levels above the saturation point.

Before starting with the experiments, the electrode contact impedances were measured for all sixteen contacts using a pulse width of 32.32 μs /phase and amplitude of 40 μA . The values were used to calculate the saturation current (μA) assuming a maximum voltage of 7.0 V. If the saturation level was exceeded, the effective stimulating current was equal to the maximum current output level for this electrode. This maximum current was used to calculate the actual σ value presented to the patient (see Table 2). To make sure there is no pollution of the results, the entire analysis in this paper was limited to data points obtained below saturation level.

Stimulation level adjustment

The Most Comfortable Loudness levels (MCLs) were determined for the primary electrode ($\sigma = 0$) and for six phantom electrode compensations ($\sigma = 0.38, 0.5, 0.63, 0.75, 0.88, 1$) at both the AS and BS locations. The subject was asked to indicate when the signal sounded most comfortably loud (MCL). Next, equal loudness contours (EqL) were obtained by balancing the loudness of a phantom electrode to a comfortably loud stimulus produced by the primary electrode alone. Two ascending and two descending tracks were used for balancing. The final result was the average of the 4 levels. The subjects listened in alternation to the stimulus from the primary electrode alone and the stimulus from the phantom electrode while they adjusted the current level of the phantom electrode stimulus in steps of 1 μA using an unmarked turning knob (Saoji and Litvak 2010). When the current level of

the primary electrode got above saturation level and therefore remained constant, the increasing levels of the compensating contacts was responsible for further loudness growth, allowing the subjects to finish the task without problems. The EqLs were used in the next experiments (pitch ranking, pitch matching).

Place pitch phantom electrode

The pitch shift was determined in two steps. First, the σ that induced the presumable lowest pitch was determined using a pitch-ranking procedure. The subject heard two sounds and was instructed to indicate the sound that was lower in pitch. The stimuli were presented at equally loud levels, using the levels determined in the EqL experiments described above. No feedback was given. The pairs consisted of two different σ 's, where a σ was compared with the neighboring higher σ and the next one in line. For example, $\sigma = 0$ was compared with $\sigma = 0.38$ and $\sigma = 0.5$ and $\sigma = 0.75$ was compared with $\sigma = 0.88$ and $\sigma = 1.00$. This resulted in eleven different comparison pairs. In the pitch ranking task, each stimulus pair was presented on eight randomized trials and subject' responses were recorded. When the stimulus with the higher σ was chosen, the answer was scored as correct. The outcome could vary between 0% and 100%. A pitch ranking score of 100% was awarded when the subject consistently identified, for example, $\sigma = 0.38$ as lower than $\sigma = 0$. A pitch ranking score of 50% was interpreted as the subject not being able to differentiate between the pair of stimuli. If the score was lower than 50% the result was interpreted as the subject perceiving the second σ as having a higher pitch, in other words a pitch reversal having taken place. The σ delivering the lowest pitch sensation was defined as the lowest value of σ from the set $[0,0.38,0.5,0.63,0.75,0.88,1]$, which is found to sound lower in pitch than both its adjacent values. This definition will always identify a σ that is below the first reversal threshold, even if the pitch is not monotonically rising for higher values of σ .

In the second step the resulting pitch shift was estimated with a pitch matching experiment. To compensate for potential errors in the first step not only the σ at first pitch reversal but also the two neighboring values were tested. For this experiment a non-marked turning knob was programmed to change the pitch of the matching stimulus. The matching stimulus could shift along the whole array using current steering with a step size of $\alpha = 0.05$. If applicable, the contacts involved in the pair would shift to the neighboring pair to allow for a continuum along the array. The MCL level for the current steering pairs was based on the monopolar MCL level of the individual contacts. Several studies validated that no current correction is needed to maintain equal loudness for the different α 's

between neighbouring contacts (Donaldson et al. 2005; Snel-Bongers et al. 2011) A loudness roving of +/-10% (in linear units, considered to be moderate) was applied to the stimulation current of the current steered stimulus in order to avoid any potential bias from a loudness cue. This current steered stimulus was generated between two adjacent electrode contacts for all the possible contact pairs, thereby making use of the earlier finding that the pitch for current steering varies monotonically with α (Snel-Bongers et al. 2011). Four tracks were performed. For the odd numbered tracks, trial 1 and 3, the pitch matching started on the contacts of the phantom pair (with current steering coefficients $\alpha=0.4$ and 0.6 respectively), while the adjacent apical electrode pair was used for the even numbered trials (with a of $\alpha=0.6$ and 0.4 respectively). The subject heard the matching stimulus and the phantom stimulus in alternation and was asked to adjust the matching stimulus to the phantom stimulus by using the unmarked turning knob.

Cochlear computer model

Model simulations of phantom electrode stimulation were performed using a computational model of the implanted human cochlea, which has been developed over the years at the Leiden University Medical Center and used to analyse stimulation paradigms such as current steering and phased array (Briaire and Frijns 2000; Briaire and Frijns 2005; Briaire and Frijns 2006; Frijns et al. 2001; Frijns et al. 2009a; Frijns et al. 2009b). The first part of the model is a volume conduction section, which employs a realistic three-dimensional representation of an implanted cochlea in order to calculate electrical potentials induced by electrical stimulation. Secondly, an active nerve fiber model simulates neural responses of 320 modelled nerve fibers to electrical stimuli. Figure 1 shows the three cochlear geometries used for this study. CM1 (Cochlear Model) and CM2 (Figures 1A and B) were based on two different histological slices of a human cochlea obtained by F. Linthicum (House Ear Institute), while CM3 (Figures 1C) was based on reconstructions from micro-CT data of a human cochlea provided by Advanced Bionics and the University of Antwerp. Generally speaking the three geometries have mostly subtle differences in the shapes of their internal structures; however there is some variability in the length of the basilar membrane, which is 35.7 mm for CM1, 32.5 mm for CM2 and 32.7 for CM3. Since CM1 and CM2 were both based on one histological slice each, the trajectories of their cochlear ducts and internal structures had to be mathematically interpolated, unlike the more accurate CM3. Apart from the size the three cochlea models differ in geometry, especially in the distance of the basal turn from the apical turns (smallest in CM2 and largest in

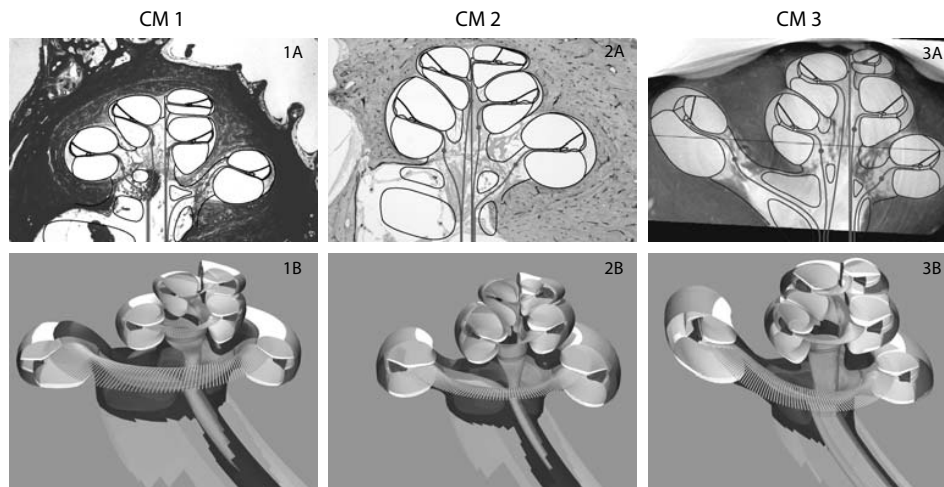


Figure 1. Illustrations of the cochlear geometries: (A) CM1, (B) CM2 and (C) CM3. The above pictures show the histological mid-modiolar cross-sections (A&B) and micro-CT reconstruction (C) used to define the geometries, along with the mesh boundaries and nerve fibres in that plane. The pictures below are ray traced images of the full 3D models. Histological slices for CM1 and CM2 were provided by F. Linthicum of the House Ear Institute, the micro-CT data for CM3 was provided by Advanced Bionics and the University of Antwerp.

CM3). Moreover, the turns are more or less stacked on top of each other in CM2, while the apical ones are more embedded in the basal turn in CM1 and CM3. Such variations are in line with the histological findings of Erixon et al. (2009), who described large variations in spiral length and also stated that each cochlea has its own 'fingerprint', an individual design with variable proportions. From previous modeling work (Frijns et al. 2001) it is expected that such anatomical differences have an impact on the outcome of cochlear implantation.

The anatomical models were implanted with realistic representations of the HiFocus-1j electrode array (Advanced Bionics, Sylmar, CA, USA) in the scala tympani. To study the effect of the distance of the electrode to the neural elements, simulations were included for electrodes in medial and lateral positions. Phantom electrode simulations were made for contacts at BS and AS, with σ -values ranging from 0 (monopolar stimulation) to 1 (bipolar stimulation) in increments of 0.1. Stimulation was applied for every value of σ , for each electrode pair. Results of the model simulations were plotted as excitation profiles: the grey shade coded maps show as a function of stimulus current which model nerve fibers were excited

and which part of the fiber was responsible for spike initiation. Every nerve fiber in the cochlear model was assigned a characteristic pitch determined by the Greenwood frequency at the location of its peripheral tip along the basilar membrane (Greenwood 1990). These values were used as the y-axis when plotting excitation profiles. The theoretically perceived pitch of a region of excited fibers was determined by its center of excitation along the basilar membrane. This was determined by calculating the center of gravity of the excited neurons (at their tips below the organ of Corti), which was in turn converted to an equivalent pitch using the Greenwood map. In this manner, excited pitch was calculated for the dynamic range of all electrode configurations. The dynamic range of a contact pair was taken to be the current range over which the stimulated nerve fibers occupied between 1 and 4 mm of the basilar membrane. For the modelling data, the current level which results in 1 mm of the basilar membrane being excited is simply referred to as threshold (Snel-Bongers et al. 2013). The current level needed to produce 4 mm of basilar membrane excitation is called $I_{4\text{mm}}$ (Briaire and Frijns 2000). To facilitate comparison between stimulus modalities, stimulus levels in the model are presented relative to the threshold for each situation. Where applicable, absolute current levels will be mentioned.

For comparison with the clinical data, a loudness correction experiment and maximal pitch shift experiment were simulated in the computational model. Additionally, the effect of current on the pitch shift was determined in the model for the σ with the largest shift.

Statistics

All statistical analysis was performed with the SPSS 16 (Statistical Package for the Social Sciences, SPSS inc., Chicago, IL) statistic software package. For the psychophysical experiments a linear mixed model (Fitzmaurice et al. 2004) and a paired sample Student's T-test were used. Differences were considered significant at the 0.05 level.

Results

Voltage compliance

The high impedance for both locations in subject S2 and S3 prevented to reach MCL level for most of the values of σ used. Therefore, these subjects were left out the analysis of all experiments (Table 2). Subjects S1, S4, S5 and S7 ran into voltage compliance limits before first pitch reversal, as shown in Table 2. These data points (mostly for apical electrode contacts) were therefore omitted from the analysis of the pitch ranking and pitch matching experiments.

Table 2. σ after recalculation with the maximum current.

σ	AS						BS					
	0.38	0.50	0.63	0.75	0.88	1	0.38	0.50	0.63	0.75	0.88	1
S1	0.38	0.50	0.63	0.75	<u>0.94</u>	0.94	0.38	<u>0.50</u>	0.63	0.75	1.06	0.85
S2	<u>0.42</u>	<u>0.68</u>	<u>0.97</u>	0.98	0.98	0.98	<u>0.45</u>	<u>0.77</u>	<u>0.93</u>	<u>0.93</u>	<u>0.93</u>	<u>0.93</u>
S3	0.38	0.50	<u>0.69</u>	1.02	1.09	1.09	0.38	0.50	<u>0.85</u>	<u>0.98</u>	<u>0.98</u>	<u>0.98</u>
S4	0.38	0.50	0.63	<u>0.56</u>	<u>0.53</u>	<u>0.53</u>	0.38	0.50	<u>0.63</u>	0.75	1.01	1.00
S5	0.38	0.50	0.63	<u>0.79</u>	<u>1.42</u>	<u>1.51</u>	0.38	0.50	<u>0.63</u>	0.75	<u>0.09</u>	<u>1.02</u>
S6	0.38	<u>0.50</u>	0.63	0.75	1.00	1.00	0.38	<u>0.50</u>	0.63	0.75	<u>0.94</u>	<u>1.02</u>
S7	0.38	0.50	<u>0.69</u>	<u>0.85</u>	<u>0.99</u>	<u>1.11</u>	0.38	0.50	0.63	<u>0.75</u>	0.88	1.00
S8	0.38	0.50	0.63	<u>0.75</u>	<u>1.19</u>	<u>1.45</u>	<u>0.38</u>	0.50	0.63	<u>0.84</u>	<u>1.05</u>	<u>1.17</u>
S9	0.38	0.50	<u>0.63</u>	0.75	<u>0.94</u>	<u>1.00</u>	0.38	0.50	0.63	<u>0.75</u>	<u>0.93</u>	<u>1.93</u>
S10	0.38	0.50	0.63	0.75	<u>0.88</u>	<u>1.01</u>	0.38	0.50	0.63	0.75	<u>0.85</u>	<u>0.85</u>

Gray square: different σ from original

underlined: σ at first pitch reversal from pitch ranking experiment.

EQL

Psychophysical experiments

The EQL results for the different values of σ normalized to the monopolar configuration of the primary electrode, are shown in Figure 2 for BS (A) and AS (B) on MCL. The individual data are plotted with a different symbol for each subject.

Several data are missing for σ 0.88 and σ 1. Because of the high impedance, it was not possible to reach MCL for these σ 's for several subjects. None of the subjects for AS were able to reach MCL level for all the σ 's and for BS 2 subjects were able to reach MCL level for all the σ 's. When using a linear mixed model, no significant difference ($p = 0.308$) was found between the two locations in the cochlea. EqL increases as the σ value increases, as shown for all the situations in Figure 2. Figure 2A includes one subject (S7), where the current first increases until $\sigma = 0.75$ and then rapidly decreases.

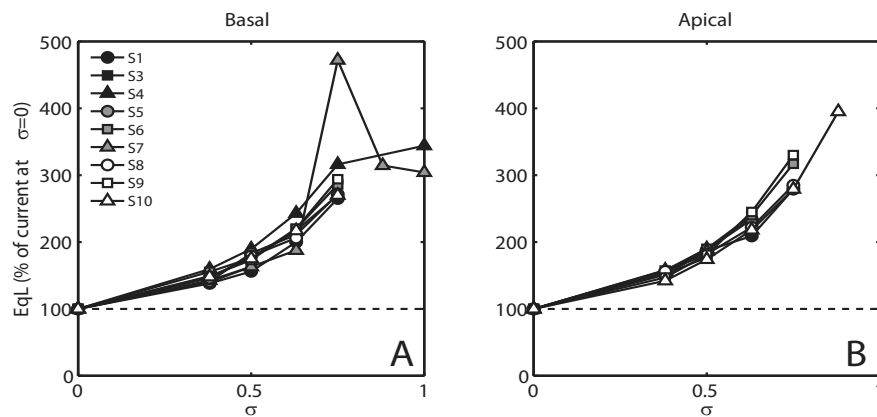


Figure 2. Individual data of the loudness correction experiment, the loudness balanced EqL (A,B) for basal (A) and apical (B) sites. The individual data are represented for each subjects with a different symbol. The different σ values are denoted on the x axis and the EqL ($MCL \sigma / MCL \sigma=0$) expressed in percentage, normalized on the 'primary' electrode ($\sigma=0$), on the y axis.

Computational model

I_{4mm} as a function of σ is shown in Figure 3 for three cochlear models (CM1, CM2, and CM3), of lateral (A, B and C) and medial (D, E and F) contacts at BS and AS. Since I_{4mm} is considered equivalent to MCL in the model, these plots can be directly compared to the EqL curves in Figure 2. In Figure 3A, B and C all curves show an increase in I_{4mm} when σ is increased starting from $\sigma=0$, which is comparable with the individual graphs from figure 2. Two curves reach a maximum at some value of σ , after which the current needed to reach 4 mm of BM excitation starts to decrease again (BS, figure 3A,C). In comparison with the clinical data, the subject

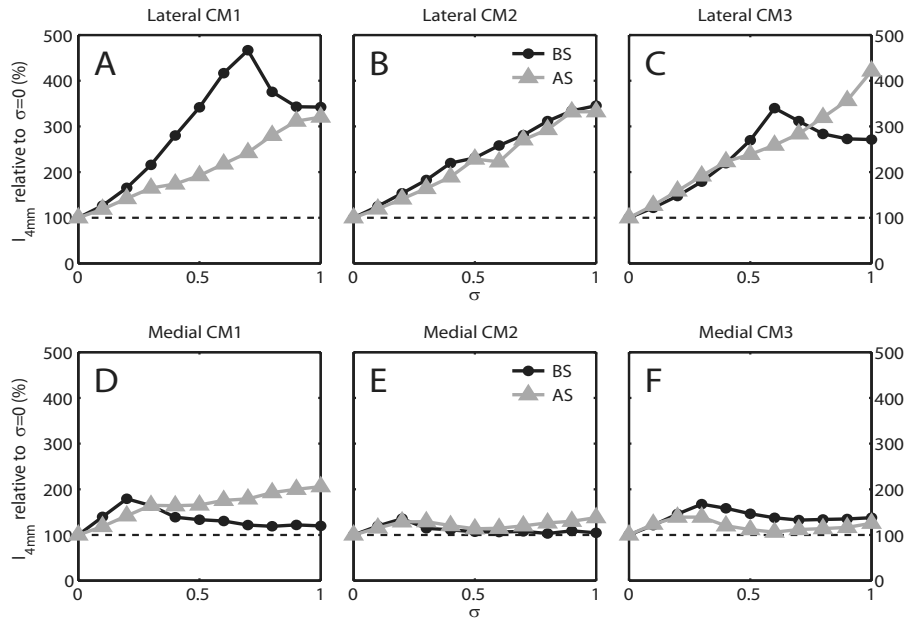


Figure 3. Curves showing the amount of current needed for phantom stimulation in order to achieve 4 mm excitation of the basilar membrane in the model. Horizontal axes indicate the value of σ , vertical axes indicate the current delivered on the main contact of the phantom electrode pair, in percentage relative to monopolar stimulation ($\sigma=0$). Black dots are for contacts at BS, grey triangles are values at AS. The left (A,D), middle (B,E) and right (C,F) graph correspond to cochlear models 1, 2 and 3 respectively. The graphs on the first line represent the data for the lateral position (A, B and C) and on the second line for the medial position (D, E and F).

(S4) illustrated with the squares (Figure 2A), also shows a small decrease, but then from $\sigma=0.88$. Subject S7 decreases from $\sigma=0.75$ for BS (Figure 2A), which almost equals CM 1 in lateral position (Figure 3A). In this model the contacts in the apical region (AS) show no decrease in $I_{4\text{mm}}$ between $\sigma=0$ and $\sigma=1$, but flatten towards $\sigma=1$, which is also seen in the clinical data. The difference between the three models can be explained by the difference in geometry. The influence of the position of the electrode array is shown in Figure 3D, E and F, where an almost flat line for the three cochlear models is demonstrated, where BS in CM1 (Figure 3D)

shows an increase at first and decreases after $\sigma=0.3$, which is also shown in CM3 for both AS and BS (Figure 3F). None of them are comparable with the clinical data.

Largest pitch shift

Psychophysical experiments

Figure 4A shows the results from one subject (S7) for stimulation site AS in a bar graph for the pitch ranking experiment. With increasing σ , a change in perception is shown. At first the larger σ of the pair (for example $\sigma=0.5$ in pair (0.38 ; 0,50)) was judged to be lower in pitch, up until $\sigma=0.63$. For larger values of σ the smallest σ of the pair was considered lower in pitch, indicating a pitch reversal. Therefore it can be inferred that $\sigma=0.63$ yielded the (first) lowest pitch sensation for this phantom

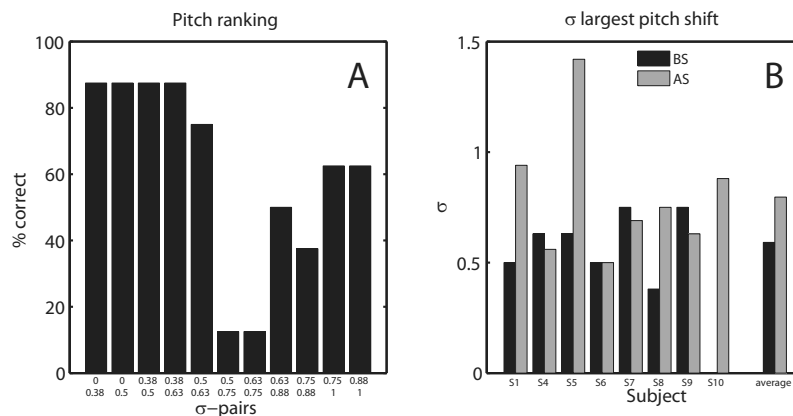


Figure 4. Data of one subjects (S7) for stimulation site AS of the pitch ranking experiment (A), with the pairs denoted on the x axis and the percentage where the lowest pitch was correctly chosen on the y axis. The individual and average data of the pitch ranking experiment (B), with the subjects denoted on the x axis and the σ at first pitch reversal on the y axis shown with the bars. The light gray bar represents the apical position and the black bar the basal position.

pair. As can be seen in Figure 4B, the σ at first pitch reversal differs between subjects. The data of S10 are missing for the basal position because the subject got tired during testing and was unable to complete the test session. In table 2 is shown that some of these σ 's at first pitch reversal (underlined) are a recalculated σ (for AS S1, S4, S5). These subjects were left out the further analysis of the pitch ranking and pitch matching experiment. In two data points subject S8 AS and S9 BS) the flanking σ is a recalculated σ . These σ are in both cases higher than the σ at first

pitch reversal. These data points can therefore be used in the pitch matching experiment.

The σ at first pitch reversal that induced a pitch shift to apical was first determined using pitch ranking measures per subject per electrode position. Results from BS were not significantly different from those obtained at AS ($p = 0.298$). First pitch reversal was obtained for a σ of 0.60 on average, which is closest to $\sigma = 0.63$, with $\sigma = 0.38$ as a minimum and $\sigma = 0.75$ as a maximum.

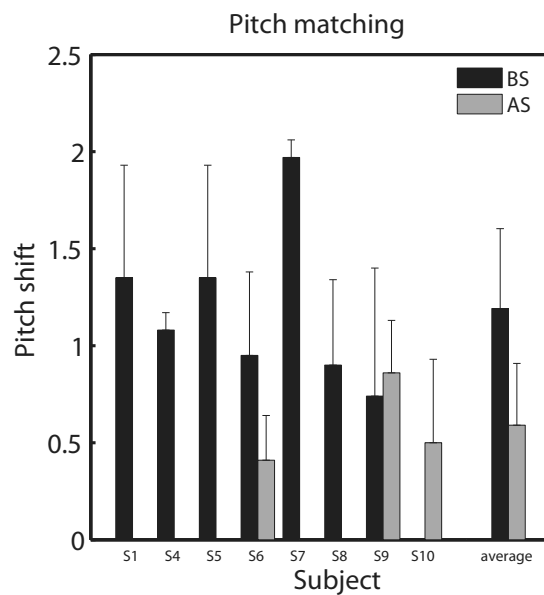


Figure 5. The individual and average data of the pitch shift at first pitch reversal experiment at MCL, with the subjects denoted on the x axis and the pitch shift expressed in electrode contact spacing on the y axis. The light gray bar represents the apical position and the black bar the basal position.

Pitch found at the σ at first pitch reversal measured with the pitch matching experiment is demonstrated in Figure 5 expressed in electrodes along the array for both AS and BS at MCL. As indicated in the material and methods, the two σ 's adjacent to the σ 's at first pitch reversal shown in Figure 4, were also tested. The figure shows the data for the σ with the pitch shift as determined by pitch matching only. This did not occur at the same σ as found in the pitch ranking experiment for all subjects. The mean shift for the σ found with the pitch ranking experiment was

0.75 electrode contacts and for the flanking σ 's respectively 0.63 and 0.52 electrode contacts. Six of the ten σ 's found with the pitch ranking experiment, had with the pitch matching experiment the largest pitch shift. In the other four cases, one of the flanking σ 's had a larger shift. All subjects showed a pitch shift in the apical direction from the apical electrode of the pair. For both locations, 2 data sets (S8 apical and S10 basal) were not collected because of subject fatigue during testing. The smallest shift was 0.41 electrode contacts and the largest shift was 1.97 electrode contacts, with a highly significant average shift of 1.07 electrode contacts ($p < 0.001$). Also the shifts per location were highly significant ($p < 0.001$): BS had an average shift of 1.19 electrode contact and AS an average shift of 0.59 electrode contact. Interestingly, also the difference between the shifts of the two locations was a highly significant ($p < 0.001$).

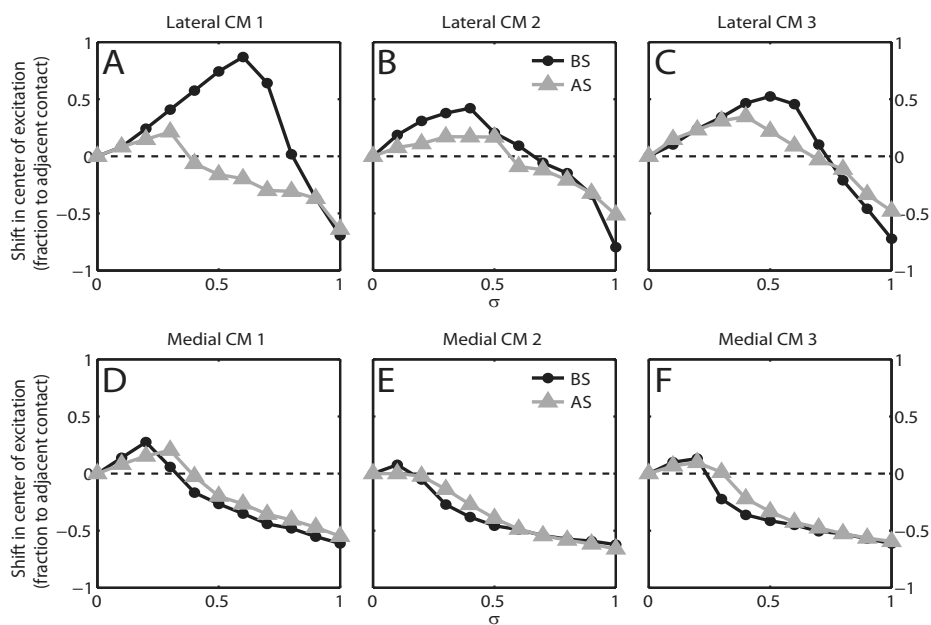


Figure 6. Pitch excited in the model with phantom stimulation as a function of σ (x axis), at I_{4mm} . On the y axis the shift of the center of excitation is shown expressed in fraction to the adjacent electrode. The largest pitch shift for the lateral (A, B and C) and medial position (D, E, and F) are shown. Black dots are for contacts at BS, grey triangles are values at AS. The left (A,D), middle (B,E) and right (C,F) graph correspond to cochlear models 1, 2 and 3 respectively.

Computational model

The simulated pitch shift (y-axis) excited at I_{4mm} is shown in Figure 6 for contacts at BS and AS in the three cochlear models for lateral and medial located electrode contacts, for varying values of σ (x-axis). The shift of the center of excitation expressed in electrode distance compared to monopolar stimulation (the horizontal dashed line) is shown on the y-axis. In all contacts there is an initial range of σ where the pitch excited by the contact decreases for increasing σ , due to the region of excitation moving in the apical direction. The largest pitch shift, approximately 1 electrode contact, is seen in figure 6A for the basal electrode contact at lateral position. The other simulations show a shift smaller than half a

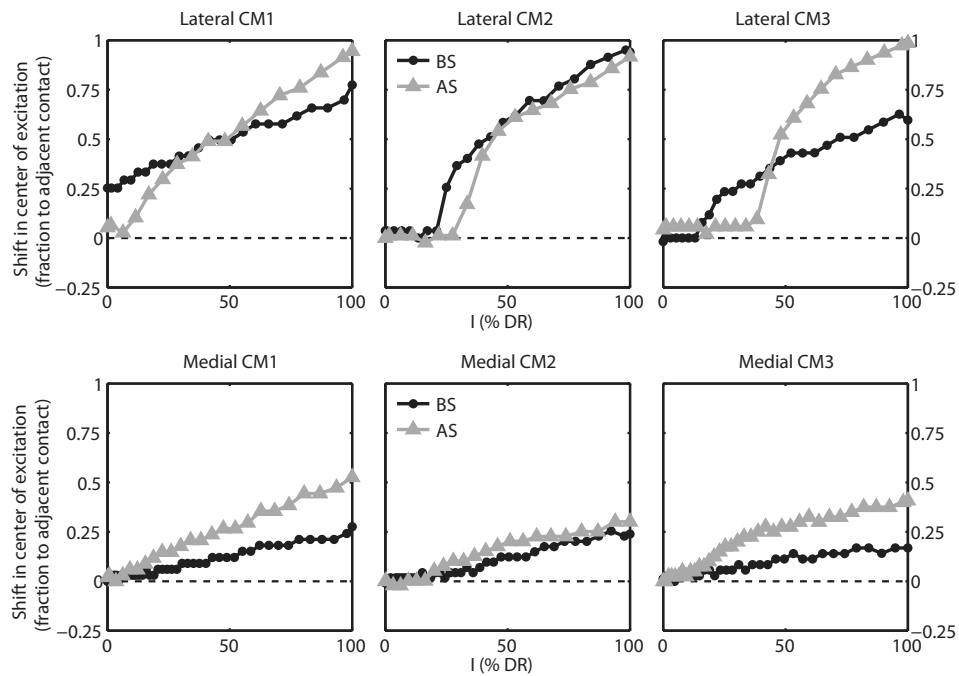


Figure 7. Model pitch excited by phantom stimulation as a function of stimulus intensity. Horizontal axes indicates the dynamic range from threshold to I_{4mm} , expressed in a percentage (0% corresponds to threshold and 100% corresponds to I_{4mm}). Vertical axis indicates the shift in center of excitation expressed in fraction to adjacent contact. Black dots are for contacts at BS, grey triangles are values at AS. The left (A), middle (B) and right (C) graph correspond to cochlear models 1, 2 and 3 respectively. The graphs on the first line represent the data for the lateral position (A, B and C) and on the second line for the medial position (D, E and F).

contact spacing. The largest pitch shift found in the psychophysical experiments was overall larger than the shift predicted by the model, although the average is comparable to cochlear model 1 in BS (Figure 6A). The apical shift is larger at BS than at AS, which was also shown in the psychophysical pitch matching data. At higher values of σ however, the center of excitation shifts more in the basal direction. The medial curves show a small shift in the apical direction with a maximum of 0.3 electrode contacts in Figure 6D for BS. Beyond $\sigma=0.2$ there is no apical shift.

In Figure 7 the pitch shift of phantom electrode stimulation in the model is plotted against stimulus level (given as percentage of the Dynamic Range (DR)), for a single value of σ with the largest pitch shift (shown in figure 6). With shift in center of excitation expressed as a fraction of the adjacent contact spacing on the y-axis, the apical and basal data can be plotted in the same graph and the difference in pitch shift becomes more easily comparable. It is immediately apparent that the shift in pitch caused by phantom electrode stimulation is dependent on stimulation level for all three cochlear models for both the lateral and medial position of the electrode contacts. Here again the shift in apical direction is larger for the lateral position than for the medial position. Also, the change in current has more influence on the shift in apical direction of the lateral position.

Excitation profiles

The computer model was used to study the relative width of the region of excitation for the various stimulus modalities and values of σ in phantom electrode stimulation. As data from the various cochlear models were not essentially different, only the data from cochlear model 1 are presented here. It also turned out that the excitation profiles for apical and basal sites were not essentially different, apart from the fact that at AS more fibers are excited in their peripheral process. Figure 8 compares monopolar stimulation on the apical contact of the pair (A), current steering for $\alpha=0.5$ (B) and phantom electrode stimulation for $\sigma=0.6$ (C)

for a lateral contact. To simplify comparison, the outline of the excitation profile in A is plotted as a grey dashed line in B and C. The center of excitation (indicated with a triangle on the vertical dashed line) for CS shifts in basal direction (B) and for phantom stimulation in apical direction (C) in comparison with monopolar stimulation. The threshold level, by definition zero dB in the graph, is higher for partial bipolar stimulation (0.66 mA) than for the monopole and CS (0.37 mA and 0.41 mA, respectively). The width of the excitation pattern of phantom stimulation is thinner than with current steering. As a result, $l_{4\text{mm}}$, as indicated by a vertical

black dashed line in Figure 8, is much higher for phantom stimulation than for the other two conditions, predicting a higher stimulus level needed to reach MCL with phantom stimulation. Although it seems from Figure 8 A and B that CS has a lower electrical dynamic range than monopolar stimulation, this varies largely between cochlear models and BS and AS. This is mainly determined by threshold variations, as the absolute value of $I_{4\text{mm}}$ is equal within 10% for both stimulus configurations in all three cochlear models, both for AS and BS.

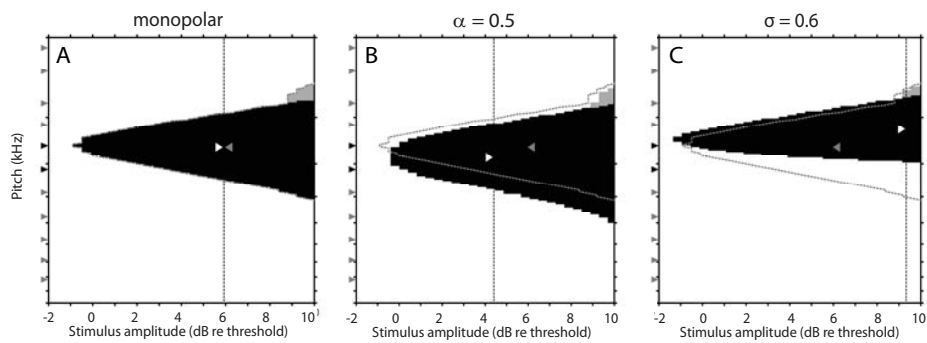


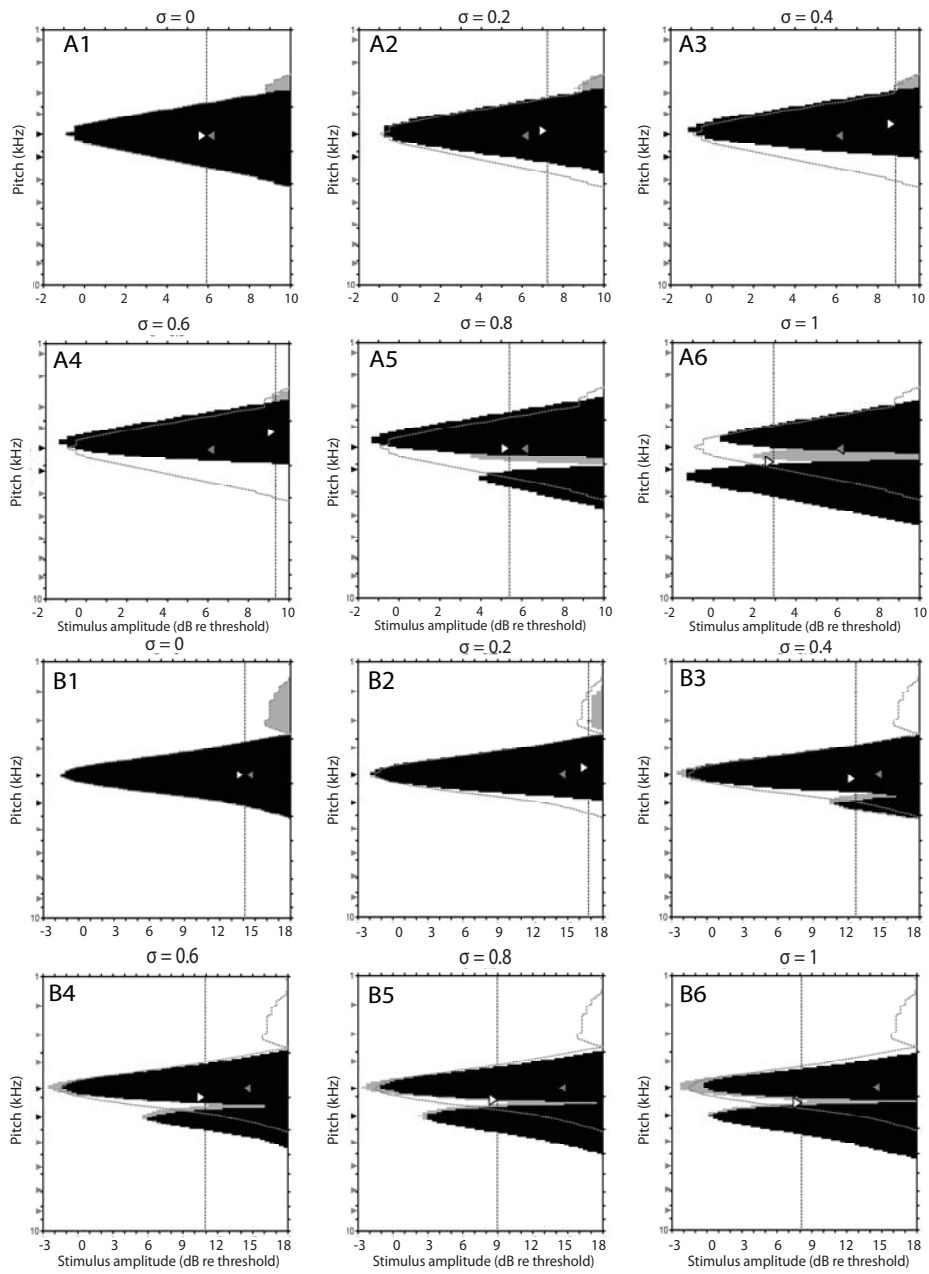
Figure 8. Excitation profiles of monopolar stimulation (A), current steering with $\alpha=0.5$ (B) and phantom stimulation with $\sigma=0.6$ (C) on a lateral contact at BS in cochlea model 1. The excitation profiles show neural stimulation patterns in a section of the cochlea for a range of stimulus levels. Horizontal axes indicate stimulation level in dB relative to threshold of the applied stimulus configuration (due to loudness differences the absolute currents varies between the graphs), the vertical axes denote the tonotopic frequencies of model fibers as determined by the Greenwood map. The triangles on the y axis denote the position of the electrode contacts. Black coloured areas indicate stimulation in the axons, grey coloured areas correspond to stimulation at the peripheral process and white areas indicate no stimulation. The vertical black dashed line in each panel marks the current level where the excited fibers occupy a total of 4 mm along the basilar membrane. The white triangle on this line indicates the center of excitation at 4 mm. The grey dashed line in each panel marks the contour of the excitation pattern and the grey triangle marks the center of excitation at 4mm of the monopolar situation.

Excitation profiles of Phantom Electrode stimulation on a lateral contact at BS are shown in Figure 9A, with different values of σ in each panel. I_{4mm} , again indicated by a vertical black dashed line in each panel, increases up until $\sigma=0.6$, after which it decreases, as has already been shown in Figure 3 (A and C). The grey dashed curve in each panel marks the contour of the excitation pattern of the monopolar situation seen in Figure 9A ($\sigma=0$). With increasing σ , the basal flank of the black area decreases. As a consequence the center of the excitation profile shifts in an apical direction, which is also indicated here with a triangle on the vertical dashed line. From $\sigma = 0.8$ onwards the excitation area of the compensating electrode appears, and the total area is broader than the excitation area of the monopolar stimulation ($\sigma=0$). At this point the center shifts back again in the basal direction and at $\sigma = 1.0$ a bipolar stimulation pattern is visible. The excitation profiles of Phantom Electrode stimulation on a medial contact at BS are shown in Figure 9B (cochlear model 1). The excitation area is smaller for $\sigma=0$ in comparison with lateral position. Further, the excitation area of the compensating electrode appears with $\sigma=0.4$, which results in a smaller to almost no shift in apical direction (Figure 6 D – F).

Discussion

This study showed that with a partial bipolar configuration, where pulses are delivered simultaneously to electrode contacts but with opposite polarity, the pitch percept is pushed away from the primary electrode contact in the contralateral direction from the compensating electrode contact. Therefore it may be possible in the future to stimulate beyond the electrode array in the apical region of the cochlea, which is in line with previous research (Saoji and Litvak 2010). The ratio σ (of current on the compensating contact to that on the primary one), which generated the pitch shift at first reversal and the place of stimulation of the phantom electrode turned out to be different across subjects. However, seven out of nine subjects were able (at a significance level of 0.05) to perceive a pitch more apical than the most apical stimulating physical contact, with a minimum shift of 0.41 electrode contacts. However, to create a phantom electrode more current correction is required to maintain equal loudness between monopolar stimulation and phantom stimulation than with current steering (Figures 2 and 3; (Frijns et al. 2009b; Snel-Bongers et al. 2011)).

Figure 9. Excitation profiles of phantom stimulation on a lateral(A) and medial (B) contact at BS in cochlea model 1, for different values of σ in each panel. The excitation profiles show neural stimulation patterns in a section of the cochlea for a range of stimulus levels. Horizontal axes indicate stimulation level in dB relative to threshold of the applied stimulus configuration (due to loudness differences the absolute currents varies between the graphs), the vertical axes denote the tonotopic frequencies of model fibers as determined by the Greenwood map. Black coloured areas indicate stimulation in the axons, grey coloured areas correspond to stimulation at the peripheral process and white areas indicate no stimulation. The vertical black dashed line in each panel marks the current level where the excited fibers occupy a total of 4 mm along the basilar membrane. The white triangle on this line indicates the center of excitation at 4 mm. The grey dashed line in each panel marks the contour of the excitation pattern and the grey triangle marks the center of excitation at 4mm of the monopolar situation seen in the upper left panel ($\sigma=0$).



EQL

The initial increase (and sometimes decrease) in current found in the psychophysical experiment determining EQL contours (Figure 2) was comparable to the results from the computational model of the cochlea for the lateral position. However, several subjects exceeded voltage compliance for the higher σ 's ($\sigma = 0.88$ and $\sigma = 1$) with our standard phase duration of 32.32 μ s. When phantom will be used in clinical practice a broader pulse is necessary for several subject to prohibit exceeding voltage compliance.

Saoji and Litvak (2010) also described an initial increase in current with σ but from $\sigma = 0.75$ a flattening of the curve. The model shows that the initial increase in current needed to achieve 4mm excitation (equal to MCL) is caused by the negative stimulus on the compensating contact (Figure 10). The negative stimulus is counteracting some of the current spread of the primary contact. This makes it more difficult for the electrical current to reach the neurons. At sufficiently high values of σ however, the amplitude of the negative stimulus becomes high enough to start exciting neurons in its own right and creates an extra area of excitation near the compensating contact (Figure 9 A5). This is essentially bipolar stimulation, and the additionally excited fibers subsequently make it easier to reach 4mm excitation. This stimulation potentially leads to a down wards slope in the EQL-curves. It appears that it highly depends on the amount of channel interaction whether this down wards slope occurs, and at which point it starts.

From both Saoji and Litvak (2010) and the present study it is clear that creating a phantom electrode at MCL is possible. The model provides insight at the point, where the apical shift became smaller with decreasing stimulus level (Figure 7) and, at the lowest levels, no shift occurred at all. From the excitation profiles in Figure 10 it is clear that for excitation around threshold level, the excitation place remains at the contact position (denoted with triangles on the y axis). The model indicates that the steering of the center of excitation is caused by a suppression of the excitation on the basal side, while the fibers at the main contact are still excited. This is achieved at the price of higher current levels needed to produce the same loudness. At low levels the number of fibers that can be suppressed on one side is smaller and thus the phantom effect is diminished.

Pitch shift at first pitch reversal

Each subject showed a pitch shift in the apical direction with increasing σ , where the extent of the shift differed from 0.41 to 1.97 times a contact spacing. Also the σ at first pitch reversal differed between subjects. The used psychophysical method to determine the largest the pitch shift is unable to detect a theoretically possible second pitch reversal with an even larger pitch shift. Only the σ at first pitch reversal and the flanking σ 's were used in the pitch matching experiment. And an possible higher pitch shift could have been missed in the current setup. The computer model, however, showed only one pitch reversal. The presented data therefore, are expected to be representative of the real pitch shift.

The computer model of the cochlea gives an explanation for this underlying mechanisms of the pitch shift. For all contacts there is an initial range of σ where the pitch excited by the contact decreases for increasing σ . The region of excitation will move in the apical direction as a result of increasing channel interaction. At higher values of σ however, the excitation pattern takes the same form as that produced by bipolar stimulation (Figure 9 A5). The additional region of excitation caused by the compensating contact shifts the center of excitation in the basal direction, increasing the excited pitch. The point at which the excitation pattern becomes bimodal is heavily dependent on the amount of channel interaction.

The pitch of phantom electrode configurations was examined in 10 subjects by Saoji and Litvak (2010). They used several pitch ranking tests to evaluate the largest pitch shift and found a shift of between 0.5 and 1.2 electrode contacts with a pitch matching experiment using monopolar stimuli on physical contacts in between a partial bipolar pair spanning several contacts. To further substantiate this outcome, the current study used, in addition to the pitch ranking test, current steering in a pitch matching procedure to determine the size of pitch shift at first pitch reversal for partial bipolar stimulation on adjacent electrodes. Moreover, the pitch matching experiment confirmed the pitch ranking data on the value of σ associated with the first pitch reversal. However, the group of subjects was small. Therefore cannot be concluded which of the two methods is most accurate.

Current steering

CS and phantom stimulation differ fundamentally from each other. Firstly in polarity of the pulses, but also in excitation profiles as shown in Figure 8. The width of the excitation profile for phantom stimulation as predicted by the model is much thinner than the profile of CS, thus providing potentially with better spatial resolution. As expected the current level to reach I_{4mm} is higher for phantom

stimulation than for the other two stimulation types. The almost equal current for monopolar stimulation and current steering is comparable with previous studies (Frijns et al. 2009b; Snel-Bongers et al. 2011; Donaldson et al. 2005).

The influence of contact position

The intended position of the HiFocus-1J electrode array is near the lateral wall of the cochlea. The psychophysical results are therefore best comparable with the computational model results of the lateral position. According to the model, however, a medial position will lead to different results, as in medial contacts, the amount of interaction between channels is less than in outer wall contacts. This is due to the closer proximity to the neurons and leads to less ‘fanning out’ of the electrical current before it reaches its target. In channels with low interaction, the compensating stimulus can excite a second region of neurons relatively independently from the primary stimulus. This is well illustrated by comparing Figures 9 A and B, where it is clear that for a peri-modiolar electrode a second lobe (basal to the main one) is elicited by the compensating current for lower values of σ than for the electrode in an outer wall position. This explains the lower values of the pitch shift in apical direction for the medial position in comparison with lateral position (Figure 6), as well as the fact that the pitch is more dependent on stimulus level for lateral positions than for medial ones (Figure 7).

Future perspectives

The phantom electrode technique works. However, more current is required to maintain equal loudness and the pitch shift at first pitch reversal differs by subject. The increase in current will lead to higher battery consumption, which can be inconvenient for CI users. Whether CI users will benefit from phantom stimulation and whether it is possible to use the phantom electrode in a speech coding strategy should be tested in a chronic clinical trial. Here speech perception scores from a normal clinical setting should be compared with speech perception scores obtained with a speech coding strategy employing phantom stimulation. In this trial it is also of importance to test whether subjects with a shallow insertion benefit from more apical stimulation. Previous studies (Hamzavi and Arnoldner 2006; Hochmair et al. 2003; Qi et al. 2011) indicated that stimulating in more apical regions enhances speech perception. They all switched off the 4 most apical electrodes in a Med-EL cochlear implant and found that the speech perception was significantly lower in this situation, than when these electrode contacts were switched on. Contrary to this finding, Gani et al. (2007) found that some patients benefit from switching off the most apical electrode contacts in a Med-EL device. Probably this is explained by

high channel interaction, which can lead to pitch confusion in the apex (Boyd 2011).

Conclusion

Based on the psychophysical data and the predictions of the computational modeling it can be concluded that phantom stimulation on an electrode array in lateral position makes it possible to stimulate more apically by about 1 electrode contact distance (1.1 mm). However, more current is required to maintain equal loudness and the model predicts that stimulating at lower current levels will probably result in a smaller pitch shift.

Reference List

Baskent, D., Shannon, R.V. (2004). Frequency-place compression and expansion in cochlear implant listeners. *J.Acoust.Soc.Am.*, *116*, 3130-3140.

Bosman, A.J., Smoorenburg, G.F. (1995). Intelligibility of Dutch CVC syllables and sentences for listeners with normal hearing and with three types of hearing impairment. *Audiology*, *34*, 260-284.

Boyd, P.J. (2011). Potential benefits from deeply inserted cochlear implant electrodes. *Ear Hear.*, *32*, 411-427.

Briaire, J.J., Frijns, J.H. (2000). Field patterns in a 3D tapered spiral model of the electrically stimulated cochlea. *Hear.Res.*, *148*, 18-30.

Briaire, J.J., Frijns, J.H. (2005). Unraveling the electrically evoked compound action potential. *Hear.Res.*, *205*, 143-156.

Briaire, J.J., Frijns, J.H. (2006). The consequences of neural degeneration regarding optimal cochlear implant position in scala tympani: a model approach. *Hear.Res.*, *214*, 17-27.

Carlyon, R.P., Macherey, O., Frijns, J.H., et al. (2010). Pitch comparisons between electrical stimulation of a cochlear implant and acoustic stimuli presented to a normal-hearing contralateral ear. *J.Assoc.Res.Otolaryngol.*, *11*, 625-640.

Donaldson, G.S., Kreft, H.A., Litvak, L. (2005). Place-pitch discrimination of single- versus dual-electrode stimuli by cochlear implant users (L). *J.Acoust.Soc.Am.*, *118*, 623-626.

Dorman, M.F., Spahr, A.J., Loizou, P.C., et al. (2005). Acoustic simulations of combined electric and acoustic hearing (EAS). *Ear Hear.*, *26*, 371-380.

Erixon, E., Hogstorp, H., Wadin, K., et al. (2009). Variational anatomy of the human cochlea: implications for cochlear implantation. *Otol.Neurotol.*, *30*, 14-22.

Finley, C.C., Holden, T.A., Holden, L.K., et al. (2008). Role of electrode placement as a contributor to variability in cochlear implant outcomes. *Otol.Neurotol.*, *29*, 920-928.

Fitzmaurice, G.M., Laird, N.M., Ware, J.H. (2004). Linear mixed effects model. In G.M.Fitzmaurice, N. M. Laird, & J. H. Ware (Eds.). *Applied Longitudinal Analysis* (pp. 187-236). John Wiley & Sons.

Frijns, J.H., Briaire, J.J., Grote, J.J. (2001). The importance of human cochlear anatomy for the results of modiolus-hugging multichannel cochlear implants. *Otol.Neurotol.*, *22*, 340-349.

Frijns, J.H., Kalkman, R.K., Briaire, J.J. (2009a). Stimulation of the facial nerve by intracochlear electrodes in otosclerosis: a computer modeling study. *Otol.Neurotol.*, 30, 1168-1174.

Frijns, J.H., Kalkman, R.K., Vanpoucke, F.J., et al. (2009b). Simultaneous and non-simultaneous dual electrode stimulation in cochlear implants: evidence for two neural response modalities. *Acta Otolaryngol.*, 129, 433-439.

Gani, M., Valentini, G., Sigrist, A., et al. (2007). Implications of deep electrode insertion on cochlear implant fitting. *J.Assoc.Res.Otolaryngol.*, 8, 69-83.

Gantz, B.J., Turner, C. (2004). Combining acoustic and electrical speech processing: Iowa/Nucleus hybrid implant. *Acta Otolaryngol.*, 124, 344-347.

Gantz, B.J., Turner, C., Gfeller, K. (2004). Expanding cochlear implant technology: Combined electrical and acoustical speech processing. *Cochlear.Implants.Int.*, 5 Suppl 1, 8-14.

Greenwood, D.D. (1990). A cochlear frequency-position function for several species--29 years later. *J.Acoust.Soc.Am.*, 87, 2592-2605.

Hamzavi, J., Arnoldner, C. (2006). Effect of deep insertion of the cochlear implant electrode array on pitch estimation and speech perception. *Acta Otolaryngol.*, 126, 1182-1187.

Hochmair, I., Arnold, W., Nopp, P., et al. (2003). Deep electrode insertion in cochlear implants: apical morphology, electrodes and speech perception results. *Acta Otolaryngol.*, 123, 612-617.

Macherey, O., Deeks, J.M., Carlyon, R.P. (2011). Extending the limits of place and temporal pitch perception in cochlear implant users. *J.Assoc.Res.Otolaryngol.*, 12, 233-251.

Oxenham, A.J., Bernstein, J.G., Penagos, H. (2004). Correct tonotopic representation is necessary for complex pitch perception. *Proc.Natl.Acad.Sci.U.S.A.*, 101, 1421-1425.

Qi, B., Liu, B., Krenmayr, A., et al. (2011). The contribution of apical stimulation to Mandarin speech perception in users of the MED-EL COMBI 40+ cochlear implant. *Acta Otolaryngol.*, 131, 52-58.

Riss, D., Hamzavi, J.S., Katzinger, M., et al. (2011). Effects of fine structure and extended low frequencies in pediatric cochlear implant recipients. *Int.J.Pediatr.Otorhinolaryngol.*, 75, 573-578.

Saoji, A.A., Litvak, L.M. (2010). Use of "phantom electrode" technique to extend the range of pitches available through a cochlear implant. *Ear Hear.*, 31, 693-701.

Skinner, M.W., Holden, T.A., Whiting, B.R., et al. (2007). In vivo estimates of the position of advanced bionics electrode arrays in the human cochlea. *Ann.Otol.Rhinol.Laryngol.Suppl.*, 197, 2-24.

Snel-Bongers, J., Briaire, J.J., van der Veen, E.H., et al. (2013). Threshold levels of dual electrode stimulation in cochlear implants. *J.Assoc.Res.Otolaryngol.*, 14, 781-790.

Snel-Bongers, J., Briaire, J.J., Vanpoucke, F.J., et al. (2011). Influence of widening electrode separation on current steering performance. *Ear Hear.*, 32, 221-229.

Snel-Bongers, J., Briaire, J.J., Vanpoucke, F.J., et al. (2012). Spread of excitation and channel interaction in single- and dual-electrode cochlear implant stimulation. *Ear Hear.*, 33, 367-376.

Turner, C.W., Reiss, L.A., Gantz, B.J. (2008). Combined acoustic and electric hearing: preserving residual acoustic hearing. *Hear.Res.*, 242, 164-171.

Verbist, B.M., Frijns, J.H., Geleijns, J., et al. (2005). Multisection CT as a valuable tool in the postoperative assessment of cochlear implant patients. *AJNR Am.J.Neuroradiol.*, 26, 424-429.

Verbist, B.M., Joemai, R.M., Briaire, J.J., et al. (2010a). Cochlear coordinates in regard to cochlear implantation: a clinically individually applicable 3 dimensional CT-based method. *Otol.Neurotol.*, 31, 738-744.

Verbist, B.M., Skinner, M.W., Cohen, L.T., et al. (2010b). Consensus panel on a cochlear coordinate system applicable in histologic, physiologic, and radiologic studies of the human cochlea. *Otol.Neurotol.*, 31, 722-730.

von Ilberg, C.A., Baumann, U., Kiefer, J., et al. (2011). Electric-acoustic stimulation of the auditory system: a review of the first decade. *Audiol.Neurootol.*, 16 Suppl 2, 1-30.

von, I.C., Kiefer, J., Tillein, J., et al. (1999). Electric-acoustic stimulation of the auditory system. New technology for severe hearing loss. *ORL J.Otorhinolaryngol.Relat Spec.*, 61, 334-340.

